

Orientational Order in Solid Ortho-Hydrogen. II. Hexagonal Close-Packed Molecular Lattice*

HUBERT M. JAMES

Department of Physics, Purdue University, Lafayette, Indiana

(Received 25 September 1967)

The orientational ordering of the molecules in solid hcp ortho-H₂ is studied theoretically, using the internal-field approximation and neglecting lattice vibrations. A relaxation method suitable for use with a high-speed computer is employed in a search for molecular orderings that might occur in stable or metastable phases; numerical characterizations of the molecular states and the thermodynamic properties of these phases are then obtained for appropriate ranges of temperature. Orders describable in terms of four or eight sublattices are studied. On the assumption that there is quadrupole-quadrupole coupling only between nearest-neighbor molecules, it is concluded that as T rises the phase (space group $Pca2_1$) stable at the lowest temperatures undergoes a first-order transition into a $P2_1/c$ phase, followed by second-order transitions into a $Pnma$ phase and then into an orientationally disordered phase. A model that includes quadrupole-quadrupole couplings between all molecules shows a first-order transition from the $Pca2_1$ phase into a $P6_3/m$ phase, followed by a second-order transition into the orientationally disordered phase. It is concluded that the "λ transition" in pure ortho-H₂ and in ortho-para mixtures sufficiently rich in ortho-H₂ will consist of a first-order transition from an orientationally ordered phase with fcc lattice ($Pa3$) to an orientationally ordered phase with hcp lattice, followed by orientational transitions on the hcp lattice that give rise to the finer structure in the specific-heat curve observed by Ahlers and Orttung. In the case of solid deuterium rich in para-D₂, one can expect the transition to be a simple one from the orientationally ordered fcc phase to an orientationally disordered hcp phase, with no fine structure in the specific-heat curve.

I. INTRODUCTION

IT has been known for many years that solid H₂ exhibits a "λ anomaly" in the specific heat that changes in magnitude and shifts in temperature with changing concentration of ortho-H₂.¹ Recent work has shown that the thermal anomaly is more complex than was previously realized. Figure 1 shows the specific heat of solid hydrogen containing 74.1% of the ortho species, as observed by Ahlers and Orttung.² In addition to the main peak, there is a small side peak, and another peak at a temperature some 0.1°K higher. The small side peak is not always evident, but the other peaks shift together in T as the ortho concentration is changed. It has also been found that the thermal anomaly is closely associated with a change in the molecular lattice from the fcc form stable at low T (provided the ortho concentration is large enough) to the hcp form stable at higher T for all ortho concentrations. The very careful work of Mills, Schuch, and Depatie³ follows the lattice change to ortho concentrations (95%) much above those at which the specific heat has been measured. Extrapolation of their results indicates that the lattice change will occur in pure ortho-H₂ at about 2.9°K.

Earlier theories of the behavior of ortho-H₂ have been based on the assumption that the molecular lattice is cubic close-packed, and that the orientational coupling is (at least primarily) the interaction of the electrostatic quadrupole moments of the molecules. Treatment of the

molecules as classical rotators⁴ shows that they pack efficiently on this lattice in a structure of high symmetry (space group $Pa3$), in which each molecule is directed along a threefold symmetry axis. James and Raich^{5,6} have shown that a quantum-mechanical treatment of this system in the internal-field approximation yields the same arrangement for the symmetry axes of the lowest orientational states of the molecules at $T=0^\circ\text{K}$; a reduction of the coupling energy by a factor 4/25 arises from the destabilizing effect of the zero-point oscillations of the molecules. Their theory indicates that this orientational ordering of the molecules in cubic ortho-H₂ would disappear in a first-order transition at 5.00°K, if one uses the commonly quoted value of the electric quadrupole moment (0.110×10^{-16} electron cm²), or at 7.51°K if one uses a value based on recent calculations (0.1348×10^{-16} electron cm²). Homma, Okada, and Matsuda⁷ have avoided the internal-field approximation, carrying out a perturbation treatment of the rotational excitations of the system of coupled rotators. They conclude that the orientational order will disappear in a first-order transition at 4.2°K. This value, apparently based on the lower value of the quadrupole moment quoted above, would be raised to 6.3°K by use of the higher value. All these calculations are based on models with a rigid molecular lattice, and their consequent neglect of the destabilizing effect of the lattice vibrations would presumably lead to excessively high

⁴ O. Nagai and T. Nakamura, Progr. Theoret. Phys. (Kyoto) **24**, 432 (1069); **30**, 412(E) (1963).

⁵ J. C. Raich and H. M. James, Phys. Rev. Letters **16**, 173 (1966).

⁶ H. M. James and J. C. Raich, Phys. Rev. **162**, 649 (1967).

⁷ S. Homma, K. Okada, and H. Matsuda, Progr. Theoret. Phys. (Kyoto) **36**, 1310 (1966); Research Institute for Fundamental Physics Report No. RIFP-62, Kyoto University, 1967 (unpublished).

* Work supported by the National Science Foundation.

¹ K. Mendelsohn, M. Ruhemann, and F. Simon, Z. Physik Chem. **B15**, 121 (1931); R. W. Hill and B. W. A. Ricketson, Phil. Mag. **45**, 277 (1954).

² G. Ahlers and W. H. Orttung, Phys. Rev. **133**, A1642 (1964).

³ R. L. Mills, A. F. Schuch, and D. A. Depatie, Phys. Rev. Letters **17**, 1131 (1966).

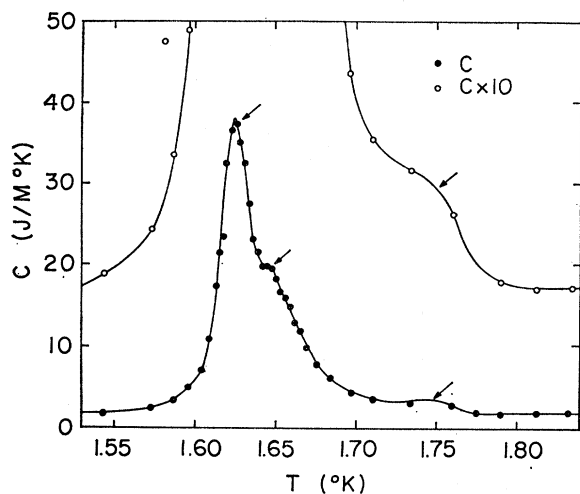


FIG. 1. The λ anomaly of solid H₂ at zero pressure and 74.1% ortho-hydrogen, as observed by Ahlers and Orttung. The arrows indicate distinguishable peaks.

computed transition temperatures. It must be emphasized, however, that the transition described by these rigid-lattice theories does not correspond to the transition that occurs in nature. When the contribution of orientational couplings is small, as in para-H₂ and orientationally disordered H₂ at high temperatures, the molecular lattice is hcp, not fcc. It is thus evident that terms of other origin in the free energy favor the stability of the hcp lattice, and that a transition from the orientationally ordered cubic phase to an orientationally disordered hexagonal phase would occur at a lower temperature than, and in preference to, a transition to an orientationally disordered cubic phase.

It is consistent with observation³ to associate the main peak in the specific heat of H₂ with the change in molecular lattice,⁸ and to attribute the additional structure in the thermal anomaly at higher T to changes in the orientational ordering of molecules on the hexagonal lattice. In the present paper, the internal-field approximation is applied to a study of the orientational ordering of ortho-H₂ molecules on a rigid hcp lattice. The techniques employed are those of the high-speed computer, rather than of mathematical analysis; the aim is to provide a survey of orientational orderings that may be of physical interest, to contribute to a general understanding of the observed phenomena, and to provide a starting point for more elaborate theoretical treatments.

The ordering of molecules with quadrupole-quadrupole couplings on a rigid hcp lattice presents a difficult problem because of the complexity of the structures that must be dealt with. Kitaigorodskii and Mirskaya⁹ made an exploratory calculation of the interaction energies of

⁸ This is possible, but not unambiguously required by the observations, which exhibit striking thermal hysteresis.

⁹ A. I. Kitaigorodskii and K. V. Mirskaya, *Kristallografiya* **10**, 162 (1965) [English transl.: *Soviet Phys.—Cryst.* **10**, 121 (1965)].

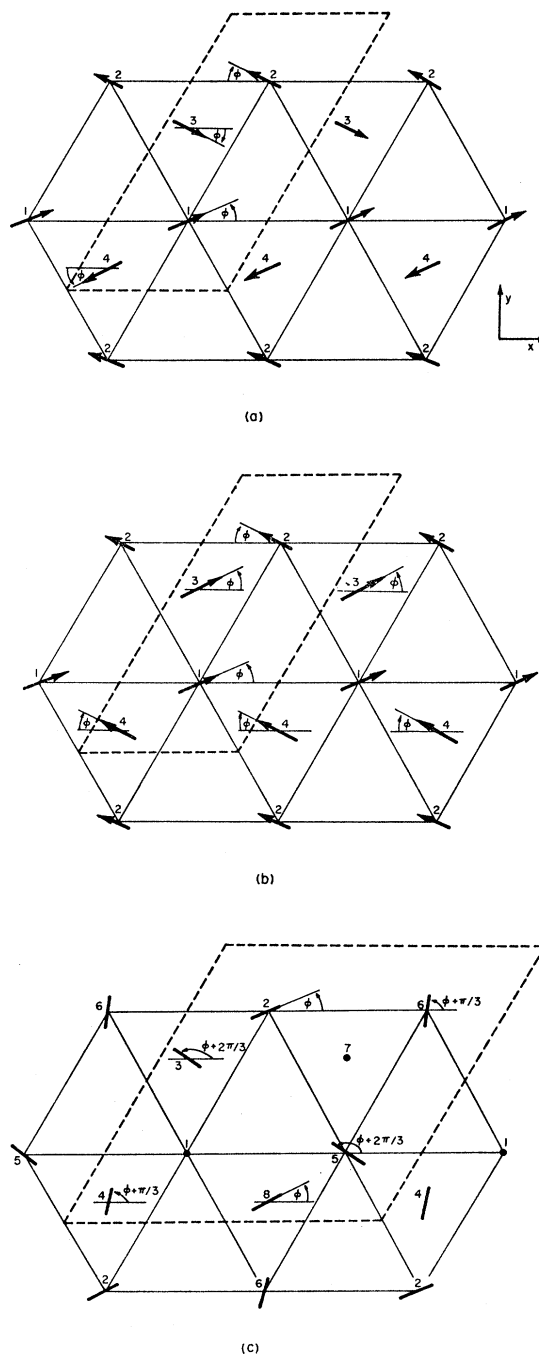


FIG. 2. Orientations of symmetry axes of molecular ground states, for various space groups. Arrows at vertices of the triangular network represent molecules in one of the hexagonal planes, seen from above; arrows at the center of triangles represent molecules in the hexagonal planes immediately above or below. The polar angle of the molecular symmetry axis with respect to the c axis of the lattice is the same for all molecules in a given figure, except that circles indicate symmetry axes parallel to the c axis. The arrowhead indicates the end of the molecule that lies above the hexagonal plane. A possible choice of unit cell is indicated by dashed lines: (a) $Pca2_1$; the space group becomes $Pbcn$ when $\varphi=0$; (b) $P2_1/c$; the space group becomes $Pnma$ when $\theta=\frac{1}{2}\pi$, $\varphi=\frac{1}{2}\pi$; (c) $P6_3/m$.

classical quadrupoles for a number of low-symmetry lattices, taking into account interactions of molecules at distances up to five times the separation of nearest neighbors. Felsteiner¹⁰ also made exploratory calculations, including interactions of molecules with separations up to 300 Å. A more systematic study has been made by Miyagi and Nakamura,¹¹ who concluded that the configuration with lowest energy is one that was previously considered by Kitaigorodskii and Mirskaya. This belongs to the orthorhombic space group $Pca2_1$, which is illustrated in Fig. 2(a). In a quantum-mechanical treatment with the internal-field approximation, the classical equilibrium orientations assume a new role as the symmetry axes of the molecular orientational distributions at $T=0^\circ\text{K}$. Miyagi and Nakamura also identified arrangements of classical quadrupoles, illustrated in Figs. 2(b) and 2(c), which make the interaction energy stationary and not far above the absolute minimum. These orientational orders also turn out to be of interest in the quantum-mechanical theory presented here.

Analytic treatment of a phase transition, even in the internal-field approximation, becomes extremely involved unless the number of independent variables, such as orientation angles, is quite small. One can reduce the number of variables by restricting attention to a particular orientational order—an order defined by specifying a system of sublattices such that all molecules on the same sublattice have identical orientational distributions, together with appropriately restrictive symmetry relations between the distributions on the different sublattices. When symmetry arguments and physical analogs are lacking, the most troublesome feature of the problem may be the decision as to what types of order need to be considered. Determination of the equilibrium orientations of the corresponding classical system provides a guide valid in the neighborhood of 0°K , but phases with other orders may come to be stable at higher temperatures. (An example of successive orientational transitions has been given by James and Keenan,¹² in the case of a model of fcc CD_4 .) It is therefore useful to carry out exploratory studies of orientational order by methods that are as nearly independent as may be of preconceptions as to the order at a given temperature. This is the advantage of the method to be described here, which yields numerical descriptions of stable and metastable phases at any chosen temperature.

The model of solid H_2 to be used here has been described previously, and the formal basis for its treatment in the internal-field approximation has been indicated.⁶ Two cases are considered:

(1) The case of quadrupole-quadrupole couplings of all pairs of molecules in the crystal: This is appropriate

¹⁰ J. Felsteiner, Phys. Rev. Letters **15**, 1025 (1965).

¹¹ H. Miyagi and T. Nakamura, Progr. Theoret. Phys. (Kyoto) **37**, 641 (1967).

¹² H. M. James and T. A. Keenan, J. Chem. Phys. **31**, 12 (1959).

if the coupling is of electrostatic origin, and if there is negligible shielding due to polarization of intervening molecules.

(2) The case of quadrupole-quadrupole coupling between nearest neighbors only: This model is suggested by the rapid decrease of quadrupole-quadrupole coupling with increasing molecular separation, possibly emphasized by shielding effects. It can also represent the effects of short-range forces, insofar as their orientational dependence simulates that of quadrupole-quadrupole couplings.

It is possible that an intermediate case will correspond most closely to reality.

Section II of this paper describes an approach to the self-consistent internal-field approximation that is appropriate for machine calculations. In Sec. III the model is treated, with both types of coupling, on the assumption that the system has the symmetry elements of the $Pca2_1$ space group. Section IV presents the results of a more general treatment of the model with nearest-neighbor coupling, and Sec. V surveys the results for the model with all molecules interacting. Finally, Sec. VI suggests a method of correlating these results with those for the fcc lattice, to arrive at a tentative picture of the over-all behavior of solid ortho- H_2 and para- D_2 .

II. DESCRIPTION OF THE RELAXATION PROCEDURE

In Reference 6, hereafter referred to as I, the internal-field treatment of ortho-hydrogen was expressed in terms of the complex surface harmonics Y_{LM} . For machine calculations it is convenient to avoid appearance of complex quantities at any point, by making use of the real surface harmonics, sometimes called components of the quadrupole moment.¹¹ We denote these by Z_τ instead of z_τ , to avoid confusion with the Cartesian coordinates. In terms of the direction cosines γ_i of the molecular axis, they are

$$\begin{aligned} Z_1 &= \frac{1}{2}\sqrt{3}(\gamma_1^2 - \gamma_2^2) \\ &= (2\pi/5)^{1/2}[Y_{2,2}(\Omega) + Y_{2,-2}(\Omega)], \\ Z_2 &= \frac{1}{2}(3\gamma_3^2 - 1) = (4\pi/5)^{1/2}Y_{2,0}(\Omega), \\ Z_3 &= \sqrt{3}\gamma_2\gamma_3 = (2\pi/5)^{1/2}i[-Y_{2,1}(\Omega) - Y_{2,-1}(\Omega)], \\ Z_4 &= \sqrt{3}\gamma_3\gamma_1 = (2\pi/5)^{1/2}[-Y_{2,1}(\Omega) + Y_{2,-1}(\Omega)], \\ Z_5 &= \sqrt{3}\gamma_1\gamma_2 = (2\pi/5)^{1/2}i[Y_{2,2}(\Omega) - Y_{2,-2}(\Omega)]. \end{aligned} \quad (1)$$

They obey the sum rule

$$\sum_{\tau} [Z_{\tau}(\Omega)]^2 \equiv 1, \quad (2)$$

and have the integral property

$$\int d\Omega Z_{\tau}(\Omega) Z_{\mu}(\Omega) = (4\pi/5)\delta_{\tau\mu}. \quad (3)$$

In terms of these functions, the coupling energy of two

TABLE I. $S(\tau, \mu; \rho) = S(\mu, \tau; \rho)$. All others are 0.

τ	μ	$\rho=$	1	2	3	4	5
1	1	$\frac{4}{3}$	0	0	0	1/18	0
1	2	0	$2/3\sqrt{3}$	0	0	0	0
1	5	0	0	0	0	0	1/18
2	2	8	0	0	0	0	0
2	5	0	0	$2/3\sqrt{3}$	0	0	0
3	3	-16/3	-4/9	0	0	0	0
3	4	0	0	4/9	0	0	0
4	4	-16/3	4/9	0	0	0	0
5	5	$\frac{4}{3}$	0	0	0	-1/18	0

equal quadrupoles Q separated by distance R_{ij} along a line with direction Ω_{ij} is

$$V_{ij}(\Omega_i, \Omega_j) = -\frac{25}{8} \Gamma_{ij} \sum_{\tau, \mu} Z_\tau(\Omega_i) K_{\tau\mu}(\Omega_{ij}) Z_\mu(\Omega_j), \quad (4)$$

where

$$\Gamma_{ij} = 6Q^2/25R_{ij}^5, \quad (5)$$

and the $K_{\tau\mu}(\Omega_{ij})$ are the functions appearing in Table II of Reference 11.

With the aid of the spherical-harmonic addition theorem, the orientational distribution of molecule j in state ν [I, Eq. (3.12)] can be written as

$$|\psi_\nu^j(\Omega_j)|^2 = \frac{1}{4\pi} + \frac{1}{2\pi} \sum_\rho Z_\rho(\Omega_j) Z_\rho(\Omega_\nu^j), \quad (6)$$

where Ω_ν^j specifies the direction of the symmetry axis of the wave function. To compute the contribution of molecule j to the effective-field potential for molecule i , one can multiply this into Eq. (4), integrate over all orientations of molecule j , and average over states ν with appropriate weights P_ν^j . The result involves the quantities

$$G(J, \mu) = \sum_\nu P_\nu^j Z_\mu(\Omega_\nu^j), \quad (\mu=1, \dots, 5). \quad (7)$$

Here the molecular index j has been replaced by the sublattice index J , since the quantities involved are the same for all molecules on the same sublattice. On further summing over all molecules $j(J)$ on sublattice J , and over all sublattices, one obtains the effective potential for molecule i :

$$U^i(\Omega_i) = -\sum_\tau Z_\tau(\Omega_i) \sum_J \sum_\mu K(I, J; \tau, \mu) G(J, \mu), \quad (8)$$

where

$$K(I, J; \tau, \mu) = \sum_{j(J)} \Gamma_{ij} K_{\tau\mu}(\Omega_{ij}) \quad (9)$$

is the same for all molecules on sublattice I . The quantities $K(I, J; \tau, \mu)$ characterize the relation between the sublattices I and J , and contain all necessary information about the geometry of the system. The five quantities $G(J, \mu)$, on the other hand, characterize the average charge distribution due to a molecule on sublattice J , and can be determined when $U^j(\Omega_j)$ is known.

The quantities $K(I, J; \tau, \mu)$ can be expressed in terms of a smaller number of geometrical constants. Let

$$\begin{aligned} D(I, J; 1) &= \sum_{j(J)} \Gamma_{ij} P_{4,0}(\cos\theta_{ij}), \\ D(I, J; 2) &= \sum_{j(J)} \Gamma_{ij} P_{4,2}(\cos\theta_{ij}) \cos 2\varphi_{ij}, \\ D(I, J; 3) &= \sum_{j(J)} \Gamma_{ij} P_{4,2}(\cos\theta_{ij}) \sin 2\varphi_{ij}, \\ D(I, J; 4) &= \sum_{j(J)} \Gamma_{ij} P_{4,4}(\cos\theta_{ij}) \cos 4\varphi_{ij}, \\ D(I, J; 5) &= \sum_{j(J)} \Gamma_{ij} P_{4,4}(\cos\theta_{ij}) \sin 4\varphi_{ij}. \end{aligned} \quad (10)$$

Then

$$K(I, J; \tau, \mu) = \sum_\rho S(\tau, \mu; \rho) D(I, J; \rho), \quad (11)$$

where the quantities S are coefficients independent of the geometry of the sublattices. They are the constants that appear in Table II of Ref. 11, and are given, for ρ up to 5, in Table I of this paper. The D 's defined in Eq. (10) are the only geometrical constants required when each sublattice is symmetric to reflection in each hexagonal plane, as in all cases considered in this paper. If one considers sublattices that lack this property, one can extend the definition of the D 's and S 's to $\rho=9$, in a way that is obvious from the structure of Table II of Ref. 11.

In Eq. (8), the effective potential for molecule i appears as a linear combination of five functions $Z_\tau(\Omega_i)$. The matrix representations of these functions in terms of the basis functions $\Phi_\alpha(\Omega)$ [I, Eq. (3.4)] are given in Table II. The matrix representation of U^i in terms of this basis is

$$[U^i] = -\sum_\tau [Z_\tau] \sum_J \sum_{\mu, \rho} S(\tau, \mu; \rho) D(I, J; \rho) G(J, \mu). \quad (12)$$

The eigenvectors of $[U^i]$ give the directions Ω_ν^i of the symmetry axes of the possible states of molecule i , and the corresponding eigenvalues are the energies ϵ_ν^i of these states, from which one can derive the values of the P_ν^i [I, Eq. (2.13)].

To find self-consistent internal fields and molecular

TABLE II. Matrix representations of the functions Z_τ in the basis Φ_α .

$\tau=1$	$\tau=2$	$\tau=3$	$\tau=4$	$\tau=5$
$\frac{1}{3}\sqrt{3} \begin{pmatrix} 1 & 1 & 0 \\ 0 & -1 & 0 \\ 0 & 0 & 0 \end{pmatrix}$	$\frac{1}{3} \begin{pmatrix} -1 & 1 & 0 \\ 0 & -1 & 0 \\ 0 & 0 & 2 \end{pmatrix}$	$\frac{1}{3}\sqrt{3} \begin{pmatrix} 0 & 0 & 0 \\ 0 & 0 & 1 \\ 0 & 1 & 0 \end{pmatrix}$	$\frac{1}{3}\sqrt{3} \begin{pmatrix} 0 & 0 & 1 \\ 0 & 0 & 0 \\ 1 & 0 & 0 \end{pmatrix}$	$\frac{1}{3}\sqrt{3} \begin{pmatrix} 0 & 1 & 0 \\ 1 & 0 & 0 \\ 0 & 0 & 0 \end{pmatrix}$

orderings, one can apply an iterative process. Having specified a system of sublattices to be considered, one can choose at random a set of values of the Ω_ν^i and P_ν^i . In general, these will not be self-consistent. Selecting a molecule i on sublattice I , one can compute $[U^i]$ by Eq. (12), and derive Ω_ν^i and P_ν^i from this. Accepting these as new and improved values for Ω_ν^I and P_ν^I , one can repeat this process for sublattice J , and for the other sublattices in turn, over and over. If this procedure leads to a stationary set of Ω 's and P 's, these will provide a self-consistent description of an orientational ordering of molecules in the crystal—in brief, of a phase. Such a limit has been approached in all calculations made by this method, except in certain cases in which there were degeneracies and the Ω_ν^I were indeterminate; even then the ϵ_ν^i approached appropriate limits. If r denotes the number of sublattices (assumed to contain equal numbers of molecules) the contribution of the orientational coupling to the internal energy per molecule can be computed as

$$U = -\frac{1}{2r} \sum_I \sum_\nu P_\nu^I \epsilon_\nu^I, \quad (13)$$

or as

$$U = -\frac{1}{4r} \sum_{I,J} \sum_{\tau,\mu} S(\tau,\mu;\rho) D(I,J;\rho) G(I,\tau) G(J,\mu). \quad (14)$$

The entropy per molecule is

$$S = -\frac{k}{r} \sum_I \sum_\mu P_\mu^I \ln P_\mu^I, \quad (15)$$

and the rotational free energy is derived from these quantities.

Such a procedure is simple but repetitive, and well adapted to machine calculation. Some comments on its convergence will be made in later sections.

The process carried out by the computer is perhaps reminiscent of the approach of artificially disoriented molecules to a natural ordering, but is more closely analogous to the relaxation process for the solution of partial differential equations. It will here be referred to as a relaxation from the initial state.

The order approached in a relaxation at any given T may depend on the initial conditions. It may be the order of lowest free energy—that of the phase stable at the given T —or another order that may be termed metastable, in that it is approached from any nearby initial conditions that can be described in terms of the *chosen sublattice structure*. Such a metastable order, found by calculations with one sublattice structure, may not appear in relaxations carried out with a less restrictive choice of sublattices; it will then be physically unstable. The relaxation process may even lead to orders that are unstable with respect to the chosen sublattice structure, if the initial conditions have some symmetry property that is maintained throughout the

TABLE III. Relations between direction cosines and the constants $G(J,\mu)$, for the space group $Pca2_1$.

Sublattice J	$\gamma_1(J)$	$\gamma_2(J)$	$\gamma_3(J)$	$G(J,1)$	$G(J,2)$	$G(J,3)$	$G(J,4)$	$G(J,5)$
1	γ_1	γ_2	γ_3	G_1	G_2	G_3	G_4	G_5
2	$-\gamma_1$	γ_2	γ_3	G_1	G_2	G_3	$-G_4$	$-G_5$
3	γ_1	$-\gamma_2$	γ_3	G_1	G_2	$-G_3$	G_4	$-G_5$
4	$-\gamma_1$	$-\gamma_2$	γ_3	G_1	G_2	$-G_3$	$-G_4$	G_5

calculation but would not be approached from initial conditions that do not possess this symmetry. For this reason, in using the relaxation process in a search for stable or metastable orders it is desirable to start from a variety of initial conditions chosen at random, with as little symmetry as is consistent with the objective at hand. It appears to be sufficient to make such trials for a relatively small number of temperatures; then, whenever a stable or metastable order is found, it can be followed through a sequence of T 's by taking the end conditions of a relaxation at one T as initial conditions for a relaxation at an adjacent T . By this method stable orders can be followed into ranges of T in which they are metastable, and conversely.

III. CALCULATIONS ASSUMING SPACE GROUP $Pca2_1$

As a simple but instructive application of the relaxation procedure, we assume that the crystal has the symmetry of the space group $Pca2_1$, with four molecules in a unit cell, as shown in Fig. 2(a). One needs four sublattices to describe this order, but the symmetry elements of the space group¹³ interchange the sublattices, and the molecules are all physically equivalent. It follows that ϵ_ν^J and P_ν^J are independent of J . The relations between the direction cosines of the symmetry axes on the several sublattices are shown in Table III. These relations are valid for the excited states as well as the ground states; in consequence, the relations between the $G(J,\mu)$ on the different sublattices are the same as those between the functions $Z_\mu(\Omega^J)$, which follow easily from Eq. (1). These relations also are shown in Table III.

Because of the symmetries of the sublattices here under consideration, $D(I,J;\rho)$ vanishes if ρ is 3 or 5, for all I and J . The terms in Eq. (12) with $\tau=1$, $\mu=2$ cancel when the summation over J is carried out. It then follows from Table I that only terms with $\tau=\mu$ enter Eq. (12), which can be written as

$$[U^i] = \sum_\tau \xi_\tau G(1,\tau) [Z_\tau], \quad (16)$$

with

$$\xi_\tau = -\frac{5}{4} \sum_J \sum_\rho S(\tau,\tau;\rho) D(I,J;\rho) \sigma(J,\rho), \quad (17)$$

where

$$\sigma(J,\rho) = G(J,\rho)/G(J,1) \quad (18)$$

¹³ There are screw axes parallel to the c axis that interchange sublattices 1 and 4, 2 and 3. Glide planes perpendicular to the x axis interchange sublattices 1 and 2, 3 and 4; glide planes perpendicular to the y axis interchange sublattices 1 and 3, 2 and 4.

TABLE IV. Coupling parameters ξ_τ/Γ , for the space group $Pca2_1$.

τ	Nearest-neighbor interactions	All interactions	
1	1.9444	1.4444 ^a	1.5041 ^b
2	11.6667	9.0000 ^a	9.0245 ^b
3	-22.2222	-27.9332 ^a	-27.9529 ^b
4	-34.4444	-31.4660 ^a	-31.4768 ^b
5	-27.7778	-30.5777 ^a	-30.5910 ^b

^a Derived from results quoted in Ref. 9.

^b Derived from lattice sums computed by Felsteiner, which include interactions of quadrupoles with separation up to 300 Å.

is +1 or -1, as indicated in Table III.

When only nearest-neighbor interactions are to be taken into account, values of ξ_τ can be obtained by a simple summation. They are given in the second column of Table IV.

To obtain values of ξ_τ for the case of all quadrupoles interacting, use has been made of computed interaction energies for classical quadrupoles. In the present case, the internal energy per molecule given by Eq. (14) can be written as

$$U = \frac{1}{2} \sum_{\tau} \xi_{\tau} [G(1, \tau)]^2. \quad (19)$$

The corresponding interaction energy in an array of classical quadrupoles with axial directions Ω_1^J can be obtained by setting $P_2^J = P_3^J = 0$, which replaces $G(1, \tau)$ by $Z_{\tau}(\Omega_1^1)$, and introducing the factor 25/4 previously mentioned. This yields

$$U(\Omega_1^1) = \frac{5}{4} \sum_{\tau} \xi_{\tau} [Z_{\tau}(\Omega_1^1)]^2. \quad (20)$$

Comparison with the results quoted by Kitaigorodskii and Mirskaya⁹ for five appropriately chosen values of $\Omega_1^1 = (\theta, \varphi)$ yields values for the ξ_τ given in the third column of Table IV. A second set of values, in the fourth column of Table IV, follows from interaction energies computed by Felsteiner.¹⁴ It is more accurate than the first set, being based on sums extended to quadrupoles separated by as much as 300 Å. The second set of ξ_τ 's has been used in deriving the results reported here.¹⁵

Since the assumption of $Pca2_1$ symmetry fixes all symmetry axes in terms of those of a single molecule, the iterative process takes on its simplest form: Assumed values of Ω_p^1 and P_p^1 determine a corresponding matrix $[U^i]$, by Eq. (16), from which one can derive new and improved values of Ω_p^1 and P_p^1 , and so on. In the present calculations this process has been carried out until the change in all quantities ϵ_r/Γ during an iteration fell below 0.00008, or up to a maximum of 300 iterations.

¹⁴ J. Felsteiner (private communication).

¹⁵ The two sets of ξ_τ 's yield results that are surprisingly similar, considering the appreciable difference in the values of ξ_1 , but the second set must be used to maintain consistency with the results reported in later sections of this paper.

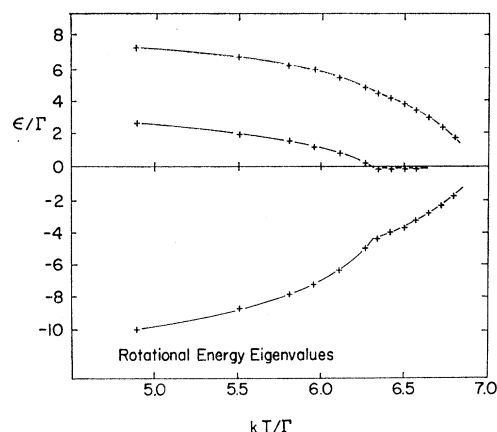


FIG. 3. Rotational energy eigenvalues computed on the assumption of $Pca2_1$ symmetry, nearest-neighbor interactions.

The calculations were made for conveniently chosen values of kT/Γ , with Γ assigned the value $0.654k$, which corresponds to the commonly used value for the quadrupole moment, $Q = 0.110 \times 10^{-16}$ electron cm². Since it appears [I, Ref. 27] that it would be more appropriate to use a larger value, $\Gamma = 0.982k$, tabular results in this paper are presented in terms of the dimensionless temperature parameter

$$t = 0.654kT/\Gamma. \quad (21)$$

Nearest-Neighbor Coupling

Calculation with nearest-neighbor couplings only were started at $t = 2.0$, with initial conditions known to solve the problem at $t = 0$. After the convergence criterion at a given t was met, calculations were started for the next higher t , with the previous solution providing initial conditions. Figures 3 and 4 show the trend of the results thus obtained. Figure 3 shows how the rotational energy levels change with T . The wide spread of the ϵ 's indicates that the effective molecular fields are far from axially symmetric. As T rises the effective field weakens and the levels draw closer together. At $t = 4.129$, $kT = 6.313\Gamma$ there is a striking discontinuity in the slopes of the ϵ curves, as well as in the plot of U shown in Fig. 4; the specific heat C (derived from the

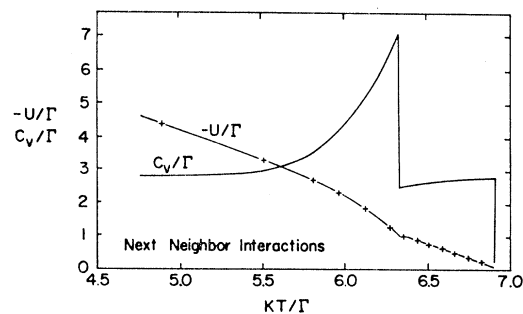


FIG. 4. Contribution of orientational coupling to the internal energy and specific heat per molecule, computed on the assumption of $Pca2_1$ symmetry, nearest-neighbor interactions.

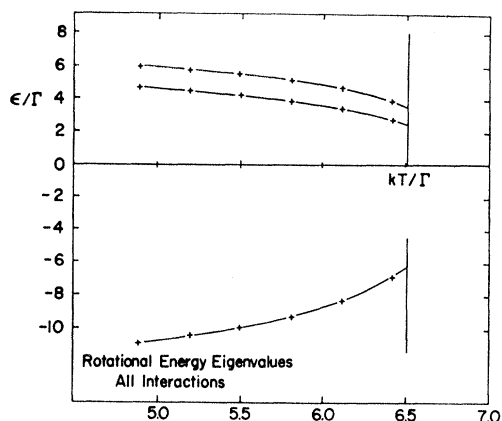


FIG. 5. Rotational energy eigenvalues computed on the assumption of $Pca2_1$ symmetry, all molecules coupled.

slope of the U curve), which has been rising rapidly, falls discontinuously. As T rises further the curves follow a different pattern, until the internal field vanishes at $t=4.51$, $kT=6.90\Gamma$, where the ϵ 's and U vanish continuously and C has a second discontinuity,¹⁶ above which the orientational coupling contributes nothing to the specific heat.

Examination of the data in Table V makes clear the reason for the first discontinuity. Table V shows, for a sequence of t 's, the number of iterations needed to meet the convergence criterion, the values of thermodynamic quantities per molecule, and then the energies and direction cosines of the symmetry axes for each of the three rotational states. As T rises from 0°K the symmetry axes of the several states shift, until at $kT=6.31\Gamma$ the symmetry axis of the first excited state lies along the y axis, and $\varphi=0$. This introduces new elements of symmetry into the structure, which comes to belong to the space group $Pbcn$. Thus there appears to be a second-order transition from the $Pca2_1$ phase to the $Pbcn$ phase at $kT=6.31\Gamma$. Data on the $Pbcn$ phase appears in the second section of Table V. It persists up to $kT=6.90\Gamma$, where it undergoes a second-order transition into the orientationally disordered phase.

The properties of the $Pbcn$ order can be followed into the range of T below the transition point. Table V contains two values thus obtained.

As one might expect from the relation between the idea of a self-consistent internal field and a variational procedure based on extremalization of F (see I), the relaxation procedure provides values of F that approach their limit much more rapidly than do the direction cosines of the symmetry axes. Another striking characteristic of the procedure, illustrated in Table V, is the increase in the number of iterations required as a second-order transition is approached.

¹⁶ Most easily located by extrapolating S to its known value for the disordered phase.

All Molecules Coupled

The results obtained using the ξ 's in the last column of Table IV, which correspond to coupling of (effectively) all molecules in the crystals, are shown in Fig. 5 and Table VI. The additional couplings change the behavior of the model in a striking way, despite the relatively small differences in the coefficients ξ . The symmetry axes of the states rotate but little as T rises, and the $Pca2_1$ order disappears abruptly in a single first-order transition to orientational disorder at $t=4.26$, $kT=6.52\Gamma$, with latent heat 1.44Γ .

It is unfortunate that the qualitative behavior of the models is so sensitive to the assumed couplings. As a result, they must be given quite separate consideration.

The results of this section do not necessarily give correct descriptions of the behavior of the models, since they are based on a particular assumption as to the symmetries of phases that may arise. Since consideration of the state stable at 0°K does not seem to be an adequate guide in such matters, the more general iterative procedure described in Sec. II has been applied. Results obtained with the two models are described in the next two sections.

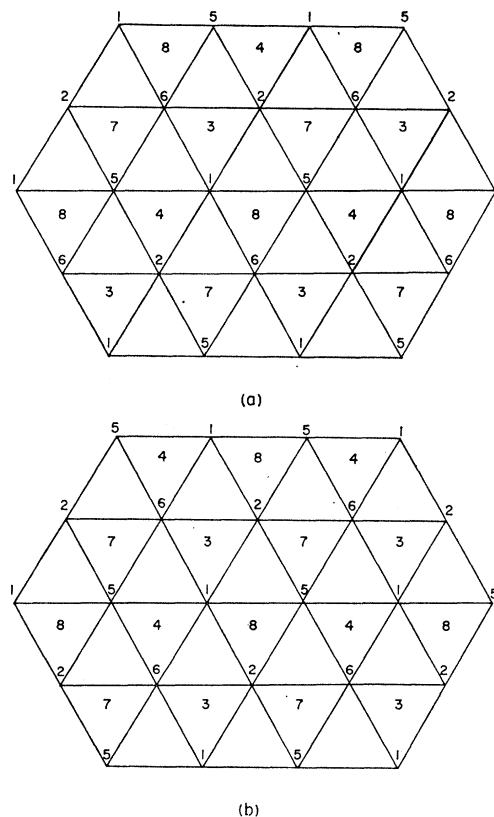


FIG. 6. Structures with eight sublattices. Numbers at the vertices of triangles represent molecules of sublattices 1, 2, 5, and 6, which lie in the same hexagonal plane. Numbers at the centers of triangles represent molecules of sublattices 3, 4, 7, and 8, which lie in the adjacent hexagonal plane above or below. (a) The sublattices have hexagonal symmetry; (b) the sublattices have tetragonal symmetry.

IV. MODEL WITH NEAREST-NEIGHBOR COUPLING

We shall here deal with the model having nearest-neighbor couplings only. The general iterative procedure has been carried out for three choices of the sublattice structure:

(1) Four sublattices, as illustrated in Figs. 2(a) and 2(b), but without any assumption concerning the relation between molecules on the several sublattices. This would permit the appearance of a wide variety of orders with 2 or 4 molecules per unit cell.

(2) Eight hexagonal sublattices, as defined in Fig. 6(a). An order with this sublattice structure is shown in Fig. 2(c).

(3) Eight tetragonal sublattices, as defined in Fig. 6(b). Any order that can be described in terms of the four-sublattice structure can be described in terms of either of the eight-sublattice structures, but not conversely. Calculations were made with the four-sublattice structure because they consume less time than those involving a larger number of sublattices.

The coupling constants required for a calculation with hexagonal sublattices are given in Table VII. Values are given only for $I=1$. One needs also to recognize the equivalences of various sublattice pairs, as regards sums over Y 's with $M+N$ even. Sublattice I is related to sublattice J in the same way that J is related to I . Also, the following pairs are equivalent:

- (a) (1,1), (2,2), (3,3), (4,4), (5,5), (6,6), (7,7), (8,8);
- (b) (1,2), (3,4), (5,6), (7,8);
- (c) (1,3), (2,4), (5,7), (6,8);
- (d) (1,4), (2,3), (5,8), (6,7);
- (e) (1,5), (2,6), (3,7), (4,8);
- (f) (1,6), (2,5), (3,8), (4,7);
- (g) (1,7), (2,8), (3,5), (4,6);
- (h) (1,8), (2,7), (3,6), (4,5).

The coupling constants for tetragonal sublattices are the same as those in Table VII, except for the vanishing of four elements with (J,τ) equal to (2,3), (2,5), (6,3), and (6,5). The equivalences of pairs of lattices, in addition to those of the pairs (I,J) and (J,I) , are as follows:

- (a) (1,1), (2,2), (3,3), (4,4), (5,5), (6,6), (7,7), (8,8);
- (b) (1,2), (3,4), (5,6), (7,8), (1,6), (2,5), (3,8), (4,7);
- (c) (1,3), (5,7), (4,6), (2,8);
- (d) (1,4), (2,3), (5,8), (6,7);
- (e) (1,5), (2,6), (3,7), (4,8);
- (f) (1,7), (2,4), (3,5), (6,8);
- (g) (1,8), (2,7), (3,6), (4,5).

The coupling constants required in the four-sublattice

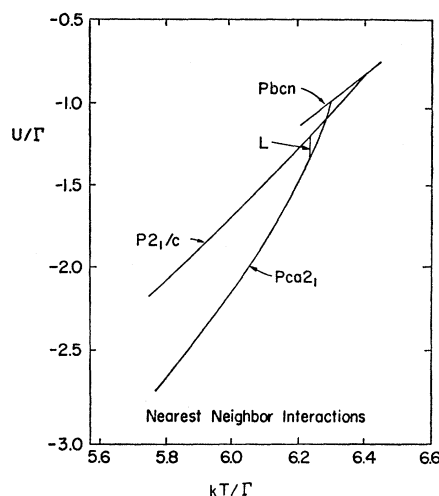


Fig. 7. Contribution of orientational coupling to the internal energy per molecule of the ordered phases of the model with nearest-neighbor interactions.

case are easily derived by noting how each of the sublattices is there made up of two of the sublattices in an eight-sublattice structure.

Starting conditions were chosen by preparing cards specifying a variety of molecular orientations, shuffling them, and then picking at random the number of these required to describe an initial configuration.

In all, 24 relaxations were carried out at $t=3.8$. With each of the three-sublattice structures described above, the $Pca2_1$ order appeared in half the cases, and a second type of order, belonging to the space group $P2_1/c$, in the other half. The symmetry axes for the molecular ground states in the $P2_1/c$ structure are arranged as shown in Fig. 2(b). Within each hexagonal layer the molecules are packed together in the same general way as in the $Pca2_1$ structure, but every second layer differs from the corresponding layer in the $Pca2_1$ structure by a reflection in the xz plane; thus the layers are packed together differently. Miyagi and Nakamura considered this order in their search for the order stable at 0°K , and found that its orientational coupling energy was about 84% of that of the $Pca2_1$ order.

The third section of Table V presents in numerical form data on this order obtained by relaxation at a sequence of increasing temperatures. Figure 7 shows its relation to the orders discussed in the previous sections, in terms of a plot of $U(T)$. In this calculation, with only nearest-neighbor interactions included, the $Pca2_1$ order is the stable one up to $t=4.083$, $kT=6.24\Gamma$, as determined by reference to the calculated values of F . There it undergoes a first-order transition into the $P2_1/c$ phase, with a small latent heat, $L=0.125\Gamma$. As T rises farther it is this phase that goes continuously into the $Pbcn$ phase in a second-order transition¹⁷ at $t=4.20$, $kT=6.42\Gamma$. Finally, as was indicated in Sec.

¹⁷ Determined by the intersection of plots of S .

TABLE VI. Data on phases appearing when all molecules are coupled. Thermodynamic functions are given on a per-molecule basis; direction cosines for molecules on sublattice 1, and for sublattice 2 in the case of $P6_3/m$.

t	Iterations ^a	U/Γ	S/k	F/Γ	Ground state			First excited state			Second excited state					
					ϵ_1/Γ	γ_1	γ_2	γ_3	ϵ_1/Γ	γ_1	γ_2	γ_3	ϵ_1/Γ	γ_1	γ_2	γ_3
<i>Pca2₁</i>																
2.0	9	-5.9031	0.0401	-6.0257	-11.9107	0.5948	0.5630	0.5739	5.3292	-0.1033	0.7614	-0.6400	6.5815	0.7972	-0.3214	-0.5110
2.4	6	-5.7146	0.0957	-6.0658	-11.7189	0.5952	0.5626	0.5738	5.2293	-0.1036	0.7618	-0.6395	6.4896	0.7969	-0.3212	-0.5117
2.8	8	-5.3740	0.1810	-6.1488	-11.3643	0.5958	0.5620	0.5737	5.0488	-0.1041	0.7624	-0.6387	6.3155	0.7963	-0.3208	-0.5128
3.2	10	-4.8349	0.2981	-6.2936	-10.7789	0.5969	0.5611	0.5735	4.7561	-0.1050	0.7632	-0.6375	6.0228	0.7955	-0.3203	-0.5144
3.6	15	-4.0328	0.4521	-6.5209	-9.8431	0.5985	0.5597	0.5733	4.2952	-0.1063	0.7647	-0.6356	5.5479	0.7941	-0.3194	-0.5171
3.8	19	-3.4954	0.5469	-6.6733	-9.1637	0.5997	0.5585	0.5731	3.9640	-0.1074	0.7659	-0.6340	5.1998	0.7930	-0.3187	-0.5193
4.0	28	-2.8214	0.6599	-6.8573	-8.2317	0.6016	0.5567	0.5729	3.5130	-0.1090	0.7677	-0.6315	4.7188	0.7913	-0.3175	-0.5225
4.1	36	-2.4034	0.7273	-6.9632	-7.5964	0.6031	0.5552	0.5727	3.2074	-0.1103	0.7691	-0.6295	4.3890	0.7900	-0.3165	-0.5251
4.2	56	-1.8824	0.8094	-7.0804	-6.7027	0.6054	0.5528	0.5726	2.7885	-0.1123	0.7715	-0.6262	3.9322	0.7879	-0.3148	-0.5292
4.25	80	-1.5380	0.8627	-7.1443	-6.0729	0.6075	0.5507	0.5725	2.4803	-0.1142	0.7738	-0.6231	3.5926	0.7861	-0.3131	-0.5329
<i>P2₁/c</i>																
3.80		-1.4167	1.0160	-6.4773	-5.2725	0.7001	0.6505	0.2945	-0.0888	0.0484	0.3682	-0.9285	5.3613	0.7124	-0.6643	-0.2263
<i>Pmma</i>																
4.00	90	-0.8802	0.9611	-6.7586	-4.1145	0.7071	0.7071	0	-0.1997	0	0	1.0	4.3142	0.7071	-0.7071	0
4.05	140	-0.7681	0.9793	-6.8328	-3.8485	Angles are constant			-0.1731	Angles are constant			4.0216	Angles are constant		
4.10	140	-0.6541	0.9976	-6.9084	-3.5567				-0.1461				3.7028			
4.15	80	-0.3520	1.0160	-6.9854	-3.2319				-0.1190				3.3509			
4.20	80	-0.4200	1.0345	-7.0637	-2.8599				-0.0921				2.9519			
4.25	60	-0.3605	1.0438	-7.1034	-2.6526				-0.0787				2.7313			
4.25	100	-0.3002	1.0531	-7.1435	-2.4233				-0.0652				2.4885			
4.275	120	-0.2394	1.0624	-7.1840	-2.1669				-0.0518				2.2187			
4.30	160	-0.1781	1.0718	-7.2248	-1.8717				-0.0383				1.9101			
4.325		-0.1164	1.0811	-7.2659	-1.5159				-0.0250				1.5408			
<i>P6₃/m</i>																
3.90	100	-1.4938	0.8617	-6.6325	-2.8655	0	0	1.0	1.5328	Indeterminate	Indeterminate	0	1.4328	Indeterminate	0	0
_b					-6.3419	0.9355	0.3533	0	0.6291	0	0	1.0	5.7128	0.3533	-0.9335	0
4.00	100	-1.1539	0.9180	-6.7686	-2.1771	0	1.0	1.0	1.0886	Indeterminate	Indeterminate	0	1.0886	Indeterminate	0	0
_b					-5.5966	0.9409	0.3387	0	0.4535	0	0	1.0	5.1431	0.3387	-0.9409	0
4.05	160	-0.9882	0.9449	-6.8398	-1.8442	0	1.0	1.0	0.9221	Indeterminate	Indeterminate	0	4.8133	Inc. terminate	0	0
_b					-5.1867	0.9438	0.3311	0	0.3733	0	0	1.0	4.8133	0.3311	-0.9438	0
4.10	220	-0.8259	0.9710	-6.9131	-1.5224	0	1.0	1.0	0.7612	Indeterminate	Indeterminate	0	0.7612	Indeterminate	0	0
_b					-4.7465	0.9462	0.3236	0	0.2992	0	0	1.0	4.4473	0.3236	-0.9462	0
4.15	100	-0.6672	0.9962	-6.9883	-1.2131	0	1.0	1.0	0.6066	Indeterminate	Indeterminate	0	0.6066	Indeterminate	0	0
_b					-4.2685	0.9488	0.3159	0	0.2314	0	0	1.0	4.037	0.3159	-0.9488	0
4.20	140	-0.5118	1.0205	-7.0654	-0.9171	0	1.0	1.0	0.4586	Indeterminate	Indeterminate	0	0.4586	Indeterminate	0	0
_b					-3.7419	0.9515	0.3078	0	0.1696	0	0	1.0	3.5692	0.3078	-0.9515	0
4.25	200	-0.3595	1.0441	-7.1443	-0.6345	0	1.0	1.0	0.3173	Indeterminate	Indeterminate	0	0.3173	Indeterminate	0	0
_b					-3.1321	0.9542	0.2993	0	0.1138	0	0	1.0	3.0183	0.2993	-0.9542	0
4.30	200	-0.2099	1.0670	-7.2250	-0.3645	0	1.0	1.0	0.1822	Indeterminate	Indeterminate	0	0.1822	Indeterminate	0	0
_b					-2.3898	0.957	0.29	0	0.0633	0	0	1.0	2.3264	0.29	-0.957	0

^a Except in the case of $Pca2_1$ order, the indicated number of iterations is for relaxation from randomly chosen initial conditions.

^b Data for sublattice 2.

TABLE VII. Values of $D(1, J; \rho)/\Gamma$ for eight sublattices, nearest-neighbor interactions. As shown, the table is for eight hexagonal sublattices. The table for eight tetragonal sublattices is the same, except that the entries for which $J=2$ or 6 and $\rho=3$ or 5 vanish.

ρ	Value of J							
	1	2	3	4	5	6	7	8
1	0	0.7500	-0.36111	-0.36111	0.75000	0.75000	0	-0.36111
2	0	7.50000	-18.33333	9.16667	-15.00000	7.50000	0	9.16667
3	0	-12.99038	0	15.87713	0	12.99038	0	-15.87713
4	0	-105.00000	23.33333	-11.66667	210.00000	-105.00000	0	-11.66667
5	0	181.86533	0	-20.20726	0	-181.86533	0	20.20726

III, the *Pbcn* phase undergoes a second-order transition into the orientationally disordered phase at $kT=6.90\Gamma$. Because of the intervention of the $P2_1/c$ phase, the specific-heat curve assumes the form shown in Fig. 8. Under experimental conditions the latent heat of the first-order transition would make a contribution to the main peak.

During a search for other orders of physical interest, 17 relaxations from randomly chosen initial configurations on the eight-sublattice structures were carried out at 4.1 and 4.15°K. All of these led to the stable $P2_1/c$ order. On the other hand, eight relaxations from configurations having approximately the character of $Pca2_1$ configurations, but not their actual symmetry, all led to the $Pca2_1$ order at 4.1°K; relaxation from the same starting configurations led to the *Pbcn* order at 4.15°K. It thus appears that these phases are metastable at the temperatures in question. In six relaxations at $t=4.2^\circ\text{K}$ only the *Pbcn* structure emerged. The orders considered by Bell and Fairbairn¹⁸ and by Danielian¹⁹ never appeared.

V. MODEL WITH ALL MOLECULES COUPLED

Results obtained for the model with all neighbors coupled will be surveyed in this section. The sublattice structures considered were those defined in Sec. IV. The coupling parameters for the eight-sublattice structures, as modified by inclusion of all couplings, are summarized in Table VIII; the constants for the four-sublattice structure can be derived from these.

The *Pbcn* phase, which played a significant role with

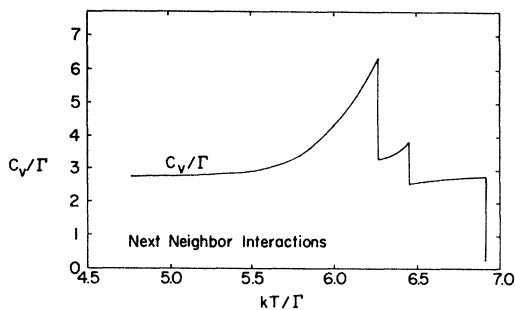


FIG. 8. Contribution of orientational coupling to the specific heat per molecule of the model with nearest-neighbor interactions.

¹⁸ G. M. Bell and W. M. Fairbairn, *Mol. Phys.* 8, 497 (1964).

¹⁹ A. Danielian, *Phys. Rev.* 138, A282 (1965).

the other model, was not found in over 40 relaxations from random configurations in the present case.

The $P2_1/c$ phase appears in somewhat modified form with the present model. It was found to be metastable at $t=3.8$, in the four-sublattice context, but as t rises θ goes to $\frac{1}{2}\pi$ and φ to $\frac{1}{4}\pi$, to give an order belonging to the space group *Pnma*. In 23 relaxations from random configurations on four sublattices and eight tetragonal sublattices, with t ranging from 4.0 to 4.2, the *Pnma* order was found in 16 cases, the $Pca2_1$ order in the rest. It did not appear at all, however, in 17 relaxations carried out from random configurations on the eight hexagonal sublattices, even though it can be described in terms of that sublattice structure. This suggests that the *Pnma* order is metastable in the tetragonal-sublattice context, but unstable in the hexagonal-sublattice context. This would mean that it is not of physical interest. Nevertheless, data on this solution of the internal field problem are included in Table VI.

A new type of order, one that cannot be described in terms of four sublattices or eight tetragonal sublattices, appeared in eight of the 17 relaxations carried out with hexagonal sublattices. In the other cases the $Pca2_1$ order resulted. This new order belongs to the hexagonal space group $P6_3/m$, and is illustrated in Fig. 2(c). Numerical data for the $P6_3/m$ phase are given in the last section of Table VI.

The $P6_3/m$ phase differs from all others considered here in that the molecules are not all physically equivalent. Two of the eight molecules in the unit cell move in internal fields with threefold symmetry axes directed along the c axis of the crystal; in the approximation of quadrupole-quadrupole couplings only there is complete axial symmetry. In consequence, the excited orientational states of these molecules are degenerate, and the orientations of the corresponding symmetry axes are indeterminate. The fields acting on these molecules are relatively weak, and the energy levels are correspondingly close together. These molecules therefore make a relatively large contribution to the entropy of the crystal, which is considerably higher than in the $Pca2_1$ phase.

Figure 9 shows the difference between the free energies (per molecule) of the ordered solutions of the internal-field problem and the free energy of the orientationally disordered phase. The $P2_1/c$ and *Pnma* phases are never stable. The $Pca2_1$ phase is stable and the $P6_3/m$ phase is (apparently) metastable up to

TABLE VIII. Values of $D(1, J; \rho)/T$ for eight sublattices, all molecules interacting.

ρ	$J=1$	2	3	5	5	6	7	8
Hexagonal sublattices								
1	0.1348	0.5104	-0.2707	-0.2707	0.5105	0.5104	-0.2638	-0.2707
2	0	4.3309	-12.0776	6.0388	-8.6617	4.3309	0	6.0388
3	0	-7.5013	0	10.4595	0	7.5013	0	-10.4595
4	0	-73.1011	6.7470	-3.3735	146.2022	-73.1011	0	-3.3735
5	0	126.6149	0	-5.8430	0	-126.6149	0	5.8430
Tetragonal sublattices								
1	0.1418	0.5104	-0.3193	-0.2707	0.5035	0.5104	-0.2152	-0.2707
2	0.1935	4.3306	-13.5790	6.0383	-8.8559	4.3306	1.5023	6.0383
3	0	0	0	10.1313	0	0	0	-10.1313
4	12.4599	-73.0918	27.4417	-3.3730	133.7570	-73.0918	-20.6954	-3.3730
5	0	0	0	-13.9394	0	0	0	13.9394

$t=4.25$, $kT=6.50\Gamma$, at which point their roles are interchanged in a first-order transition with latent heat 1.24Γ . The $P6_3/m$ phase passes into the orientationally disordered phase in a second-order transition at²⁰ $t=4.37$, $kT=6.68\Gamma$. The specific heat behaves as shown in Fig. 10; in an experimental situation the latent heat of the first transition would presumably appear as a contribution to the main peak.

Miyagi and Nakamura¹¹ considered the $P6_3/m$ order in their search for the order stable at 0°K , and found that its internal coupling energy was about 90% of that of the $Pca2_1$ phase. The present calculation shows that as T rises the internal energy of the $P6_3/m$ phase remains considerably higher than that of the $Pca2_1$ phase, but that its larger entropy eventually causes its free energy to fall below that of the $Pca2_1$ phase, so that it becomes stable. Similar behavior was indicated by internal-field calculations¹² on cubic CD_4 , which predicted that, with rising T , a high-entropy phase would become more stable than the phase with lowest U .²¹ On the other hand, in the case of the model of H_2 considered

in Sec. IV, the $P2_1/c$ phase appeared primarily because its internal energy decreased with respect to that of the $Pca2_1$ phase.

VI. CONCLUSION

It cannot be excluded that there are other stable orderings of molecules with larger unit cells than those considered in the present work. Attention has been limited to orders in which the unit cell extends only through two hexagonal planes, and the molecules on any hexagonal plane lie between two neighboring hexagonal planes that have their molecules ordered in exactly the same way. This may be too restrictive. At any rate, it is evident that with either model of hexagonal ortho- H_2 one can expect several orientational transitions to occur.

The over-all problem of the transitions in ortho- H_2 will now be considered in terms of the model with all molecules coupled. For the phases of hexagonal ortho- H_2 , Fig. 9 shows only the contribution of the orientational couplings to the free energy of the model. The total free energy of the real crystal includes other terms that depend on whether the lattice is cubic or hexagonal close-packed: those arising from radial forces between molecules that are not nearest neighbors, from three-body interactions, and from lattice vibrations. Because of the large amplitude of the lattice vibrations and the anharmonic binding in H_2 , one can expect the last of

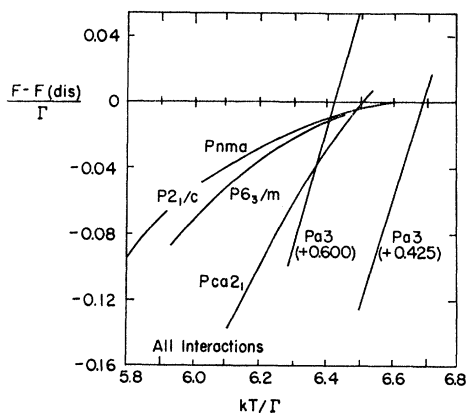


FIG. 9. Contribution of orientational coupling to the free energy per molecule of the model with all molecules coupled. The differences between the free energies of the ordered and disordered phases are shown; in the case of the $Pa3$ phase of cubic ortho- H_2 there is an added constant, as indicated.

²⁰ As determined by extrapolating plots of S or U , which are very nearly linear up to $t=4.325$.

²¹ R. L. Mills (private communication).

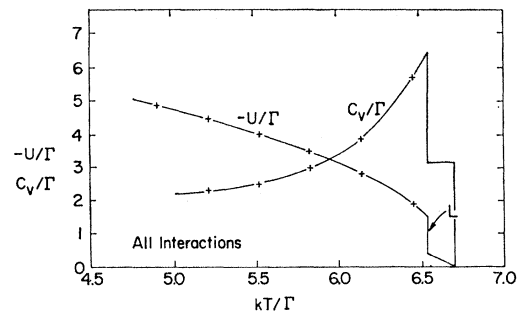


FIG. 10. Contribution of orientational coupling to the internal energy U and specific heat C_v of the model with all molecules coupled.

these factors to be particularly important. Their net effect can be deduced from the case of para-H₂, in which the effect of orientational couplings is relatively small: They tend to stabilize the hexagonal lattice. In ortho-H₂, on the other hand, the orientational contributions favor stability of the cubic lattice. In picturesque terms, the ortho-H₂ molecules pack together better on a cubic lattice, and thus favor its stability. The lattice change in ortho-H₂ takes place when these factors balance each other. In Fig. 9 there are two curves representing the free energy of the cubic phase with space group *Pa3*, in which a constant has been added to the computed orientational terms to represent the difference in the free energy due to the other terms mentioned above. We consider first the one of these on the left. Its relation to the curves for the hexagonal phases would imply that the cubic *Pa3* order is stable up to about $kT=6.36\Gamma$, at which point there is a first-order transition to the hexagonal *Pca2*₁ order. This is followed at $kT=6.5\Gamma$ by another first-order transition to the hexagonal *P6*₃/*m* order, which finally disappears at $kT=6.68\Gamma$ in a second-order transition to orientational disorder on an hcp molecular lattice. This sequence of events would yield a thermal behavior that is about what one would expect from the rather wide extrapolation of the data of Ahlers and Orttung to pure ortho-H₂. The details of this behavior are, of course, only very tentatively indicated by the present calculations.

To the approximation of the present treatment, the orientational contributions to the free energy of para-D₂ would be the same as for ortho-H₂. The lattice vi-

brational terms in the free energy, particularly those due to the anharmonic coupling, will be much reduced because of the smaller amplitude of the lattice vibrations. The second *Pa3* curve in Fig. 9 shows that such a reduction could easily produce a shift of the lattice change to a temperature above that at which any orientational order is retained on the hexagonal lattice. Extrapolation of the observations of Mills, Schuch, and Depatie¹² indicates that the lattice transition in para-D₂ will occur about 1.0°K above the lattice transition in ortho-H₂. This difference is considerably greater than the range in which the other thermal features are observed in 74% ortho-H₂. Since this range does not seem to broaden as the composition of the ortho-para mixture is changed, one is led to the conclusion that in pure para-D₂ there will be a single transition from the *Pa3* order on the cubic lattice to orientational disorder on a hexagonal lattice. This is consistent with the apparent absence of thermal structure in the observed specific heat of mixtures of ortho- and para-D₂.²²

ACKNOWLEDGMENTS

The author wishes to express appreciation for the hospitality of the Physics Department and the Institute of Computer Science of the University of Toronto during the period in which much of this work was done. He is also indebted to Joshua Felsteiner for computation of lattice sums used in deriving the coupling constants in Table VIII.

²² G. Grenier and D. White, *J. Chem. Phys.* **40**, 3015 (1964).